Forest fires and other examples of self-organized criticality

1996 J. Phys.: Condens. Matter 8 6803

(http://iopscience.iop.org/0953-8984/8/37/004)

J. Phys.: Condens. Matter **8** (1996) 6803–6824. Printed in the UK

REVIEW ARTICLE

Forest fires and other examples of self-organized criticality

Siegfried Clar, Barbara Drossel and Franz Schwabl

Institut für Theoretische Physik, Physik-Department der Technischen Universität München, James-Franck-Strasse, D-85747 Garching, Germany

Received 9 May 1996

Abstract. We review the properties of the self-organized critical (SOC) forest-fire model. The paradigm of self-organized criticality refers to the tendency of certain large dissipative systems to drive themselves into a critical state independent of the initial conditions and without fine tuning of the parameters. After an introduction, we define the rules of the model and discuss various large-scale structures which may appear in this system. The origin of the critical behaviour is explained, critical exponents are introduced and scaling relations between the exponents are derived. Results of computer simulations and analytical calculations are summarized. The existence of an upper critical dimension and the universality of the critical behaviour under changes of lattice symmetry or the introduction of immunity are discussed. A survey of interesting modifications of the forest-fire model is given. Finally, several other important SOC models are briefly described.

1. Introduction

Driven dissipative systems far from thermodynamic equilibrium show a rich variety of patterns. Since they receive a permanent input of energy, they can maintain states which are highly ordered or complex. Ubiquitous examples for complex structures are 'fractals' [1, 2] as well as their temporal counterpart, '$1/f$-noise' [3, 4]. Fractals are self-similar structures that look the same on different scales of observation, since they have no intrinsic length scale. Their spatial correlation functions are power laws. Well known examples are mountain landscapes and coastlines. $1/f$-noise is the temporal equivalent of fractals. Its name indicates that the Fourier transform of the temporal correlation function is a power law of the form $1/f^{\alpha}$ with $\alpha \approx 1$. Like fractals, $1/f$-noise can be found in many natural systems, e.g. undersea ocean currents or stock market prices.

In 1987, Bak, Tang and Wiesenfeld introduced the 'sandpile model' which evolves into a critical state irrespective of initial conditions and without fine tuning of parameters [5, 6]. Such extended non-equilibrium systems are called 'self-organized critical' (SOC) and exhibit power-law correlations in space and time. The concept of SOC (for a review see [7]) has attracted much interest since it might explain part of the abundance of fractals and $1/f$-noise in nature and create a link between the two. Models for earthquakes [8, 9], the evolution of populations [10, 11], the formation of clouds [12] and river networks [13], and many more have been introduced and investigated mainly by computer simulations, but with few exceptions, most of these SOC models are still barely understood.

This review is mainly devoted to the 'forest-fire model' (FFM) [14], which is a particularly simple example for open systems which shows nevertheless a variety of different structures, depending on the parameters. In the limit of a double separation of time scales, the FFM becomes SOC, with a power-law distribution of fires and forest clusters.

0953-8984/96/376803+22$19.50

The FFM is a stochastic cellular automaton which is defined on a d-dimensional hypercubic lattice with L^d sites. Each site is occupied by a tree, a burning tree, or it is empty. During one time step, the system is parallely updated according to the following rules

(i) Burning tree $\longrightarrow$ empty site.
(ii) Tree $\longrightarrow$ burning tree with probability $1-g$ if at least one nearest neighbour is burning.
(iii) Tree $\longrightarrow$ burning tree with probability f if no nearest neighbour is burning.
(iv) Empty site $\longrightarrow$ tree with probability p.

An important application of the FFM comes from its close relation to excitable media [15], which comprise phenomena so varied as spreading of diseases, oscillating chemical reactions, propagation of electrical activity in neurons or heart muscles, spiral galaxies and many more (for a review on excitable systems see e.g. [16, 17]). These systems essentially have three states which are called quiescent ($\triangleq$ tree), excited ($\triangleq$ burning tree) and refractory ($\triangleq$ empty site). Excitation spreads from one place to its neighbours if they are quiescent. After excitation, a refractory site needs some time to recover its quiescent state. Since excitable systems are often deterministic, it is, however, not always possible to describe their behaviour in the framework of the FFM, where some of the parameters are stochastic.

Turning back to the FFM, we consider a system with arbitrary initial conditions. After a transition period the system approaches a steady state the properties of which depend only on the parameter values. If the system size L is large enough the properties of the steady state are also independent of the boundary conditions. Let ρ_e, ρ_t, and ρ_f be the mean density of empty sites, of trees and of burning trees in the steady state. These densities are related by the equations

$$\rho_e + \rho_t + \rho_f = 1 \tag{1.1}$$

and

$$\rho_f = p\rho_e. \tag{1.2}$$

The second relation says that the mean number of growing trees equals the mean number of burning trees in the steady state. Depending on the magnitude of the parameters, a variety of large scale structures arise.

1.1. Fire fronts and spirals

In the limit of slow tree growth p and without lightning and immunity, fire only spreads from burning trees to their neighbours but does not occur spontaneously. In this version, which was originally introduced by Bak *et al* [18], the fire fronts become more and more regular and spiral-shaped with decreasing p [19]. A snapshot of this state is shown in figure 1. A more thorough analysis of the spatial and temporal correlations in the system revealed the existence of characteristic length and time scales proportional to $1/p$, both of which become increasingly distinct with decreasing p [20], indicating increasing determinism in this limit. Spiral waves are very familiar in excitable media and have been observed in oscillating chemical reactions, the heart muscle, and the chemical signals of the amoeba *dictyostelium discoideum* [16, 17]. It is also known that certain epidemics occur periodically [16]. They already occur in simple deterministic versions of the FFM [21].

1.2. Percolation due to immunity

When the immunity is non-zero, the fire fronts present for $g = 0$ become more and more fuzzy with increasing immunity g, and the forest becomes denser [15]. At a critical value

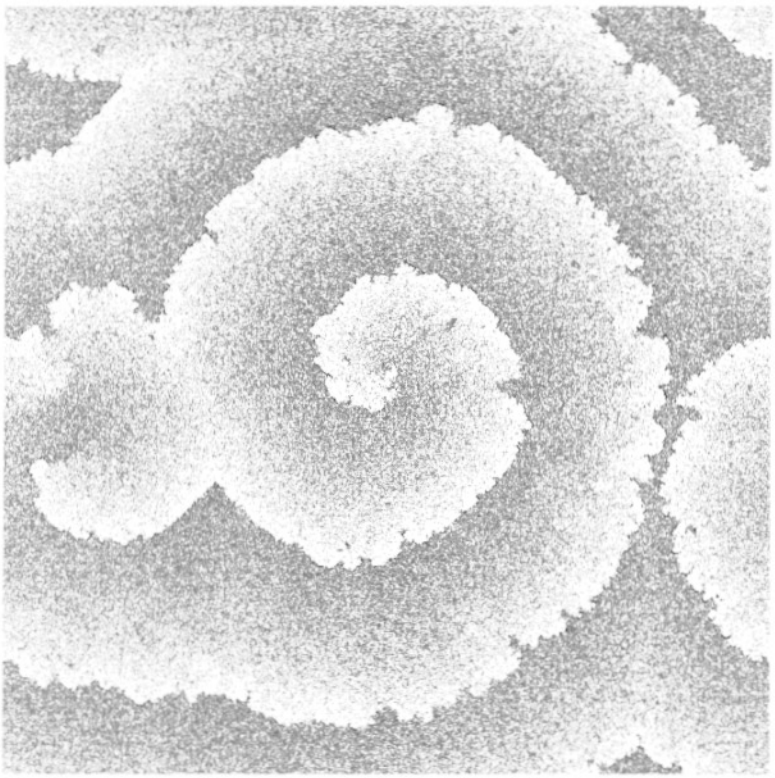

Figure 1. Snapshot of the Bak *et al* forest-fire model in the steady state for $p = 0.005$ and $L = 800$. Trees are grey, burning trees are black, and empty sites are white.

$g = g_C(p)$ the fire density becomes zero and the forest density becomes one. Figures 2 and 3 show two snapshots of the system for values of g far below $g_C(p)$ and near $g_C(p)$. At $g_C(p)$, the fire just percolates through the system. Since sites are not permanently immune, this kind of percolation is different from usual site percolation and is in the same universality class as directed percolation in $d+1$ dimensions (the preferred direction corresponds to the time) [22]. The critical immunity $g_C(p)$ increases with increasing p, since the fire then can return sooner to sites where it already has been. Above $g_C(p)$ the steady state of the system is a completely dense forest. A similar model, using the language of spreading diseases has been studied independently in [23].

1.3. Self-organized critical (SOC) behaviour

The SOC behaviour occurs when the lightning probability is non-zero. For simplicity, we set the immunity to zero, but we will show later that the SOC state persists for $g > 0$. The ratio p/f is a measure for the number of trees growing between two lightning strokes and therefore for the mean number of trees destroyed per lightning stroke. In the limit

$$f \ll p \tag{1.3}$$

there exist consequently large forest clusters and correlations over large distances. The model is SOC when tree growth is so slow that fire burns down even large clusters before

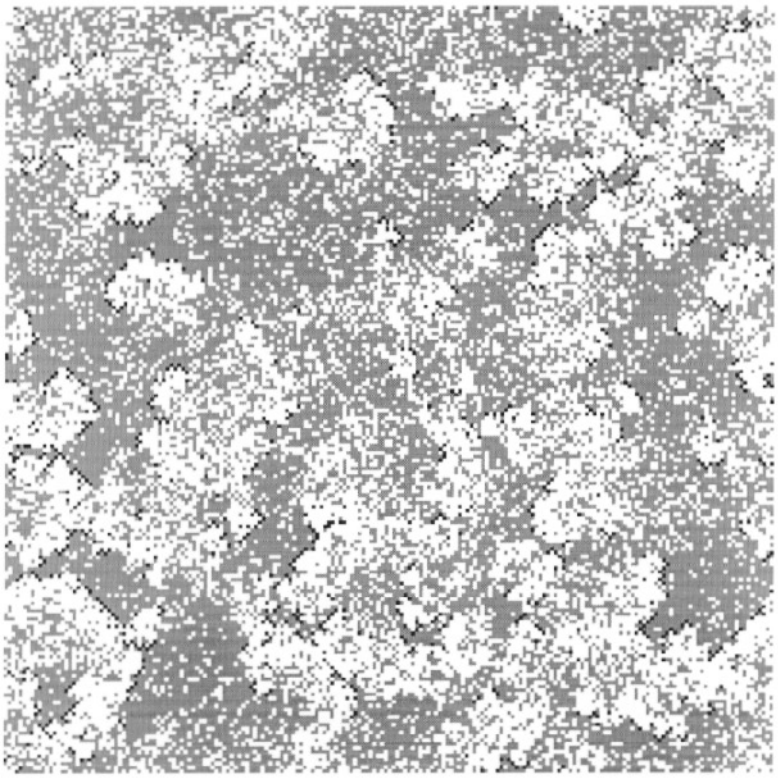

Figure 2. Snapshot of the forest-fire model far below the critical immunity for $g = 0.2$, $p = 0.05$, and $L = 200$. Trees are grey, empty sites are white, and burning trees are black.

new trees grow at their edge. This condition, which assures invariance under a change of the length scale, reads

$$p \ll T^{-1}(s_{\max}) \tag{1.4}$$

where $T(s_{\max})$ is the time the fire needs to burn down a large forest cluster. It diverges in the limit $f/p \to 0$ according to $T(s_{\max}) \propto (f/p)^{-\nu'}$, with an appropriate exponent ν'.

In this case, the dynamics of the system depend only on the ratio f/p, but not on f and p separately. When f and p are both decreased by the same factor, the overall time scale of the system is also changed by this factor, but not the number of trees that grow between two lightnings and therefore not the size distribution of forest clusters and of fires. In the simulations, the condition (1.4) is most easily realized by burning forest clusters instantaneously, i.e. during one time step. This extreme limit of the SOC forest-fire model has been invented independently by Henley [24].

The inequalities (1.3) and (1.4) represent a *double separation of time scales*

$$(f/p)^{-\nu'} \ll p^{-1} \ll f^{-1} \tag{1.5}$$

which is the condition for SOC behaviour in the FFM. The time in which a forest cluster burns down is much shorter than the time in which a tree grows, which again is much shorter than the time between two lightning occurrences. Separation of time scales is quite frequent in nature, while the tuning of parameters to a certain finite value only takes place

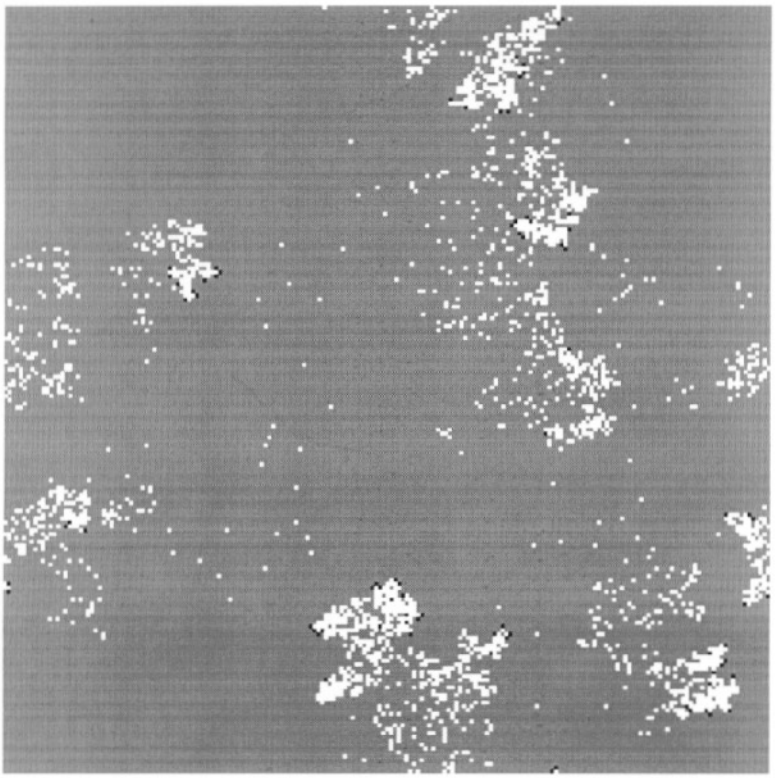

Figure 3. Snapshot of the forest-fire model near the critical immunity for $g = 0.48$, $p = 0.05$, and $L = 200$. Trees are grey, empty sites are white, and burning trees are black.

accidentally. Thus, the FFM is critical over a wide range of parameter values. A snapshot of the critical state is shown in figure 4.

In the following, we will mainly discuss the properties of the SOC FFM, and we will compare this model to other SOC systems, as there are e.g. the sandpile model, the earthquake model, etc. The outline of the remainder of this paper is as follows: In section 2.1, the critical exponents of the forest-fire model are defined, and scaling relations between them are derived. Section 2.2 presents the results of computer simulations and discusses the issue of universality of the critical behaviour. Section 2.3 deals with the analytical results including renormalization group approaches. In section 3, several modifications of the forest-fire model are discussed. Some of the most prominent other SOC systems are presented in section 4. Section 5 contains concluding remarks.

2. The self-organized critical forest-fire model

2.1. Critical exponents and scaling relations

In this section, we consider some principal properties of the SOC FFM which will lead us to the definition of critical exponents and the derivation of scaling relations between them. In the following, we restrict ourselves to the case $g = 0$.

The mean number $\bar{s}$ of trees that are destroyed by a lightning strike can be calculated

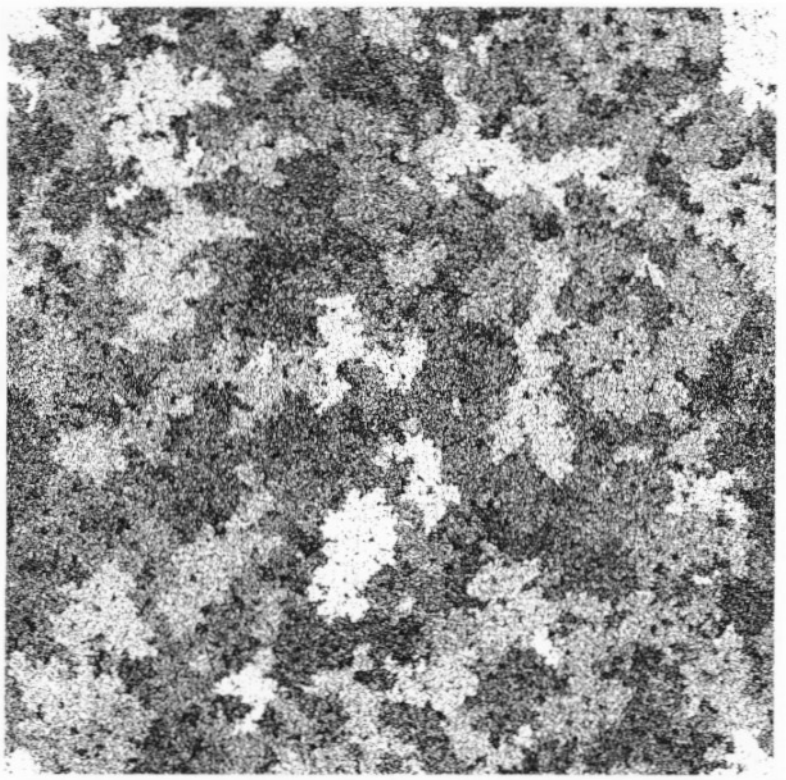

Figure 4. Snapshot of the SOC state in 2 dimensions. Trees are black, empty sites are white. The parameters are $L = 1024$ and $f/p = 1/500$.

as follows. During one time step, there are $f\rho_t L^d$ lightning strokes in the system and $p\rho_e L^d$ growing trees. In the steady state, the number of growing trees equals the number of burning trees, and therefore the mean number of trees destroyed by a lightning strike is

$$\bar{s} = \frac{p\rho_e}{f\rho_t} \simeq \frac{p}{f}\frac{1-\rho_t}{\rho_t}. \tag{2.1}$$

In the last step, the fire density which is very small due to time scale separation was neglected. For small values of f/p, the forest density ρ_t approaches a constant value. If this constant value is less than 1, the second factor on the right-hand side of equation (2.1) is also constant for small f/p, and equation (2.1) then represents a power law

$$\bar{s} \propto (f/p)^{-1}. \tag{2.2}$$

In $d \geqslant 2$ dimensions, the critical forest density

$$\rho_t^c = \lim_{f/p \to 0} \rho_t$$

in fact, must be less than 1, as the following consideration indicates: if the critical forest density were $\rho_t^c = 1$ in $d \geqslant 2$ dimensions, ρ_t would be very close to 1 for small values of f/p. Then the largest forest cluster would contain a non-vanishing percentage of all trees in the system, and the average number $\bar{s}$ of trees burned by a lightning strike would diverge in the limit $L \to \infty$ with fixed f/p, in contradiction to equation (2.1). In one dimension, there is no infinitely large forest cluster in the system as long as $\rho_t < 1$, and therefore the

critical forest density is $\rho_t^c = 1$. Nevertheless equation (2.2) holds also in 1 dimension since the forest density approaches its critical value only logarithmically slowly, as will be shown in subsection 2.3. equation (2.2) indicates a critical point in the limit $f/p \to 0$. Close to this critical point, i.e. if $f \ll p$, there is scaling over many orders of magnitude.

Let $n(s)$ be the mean number of forest clusters per unit volume consisting of s trees. Then the mean forest density is

$$\rho_t = \sum_1^\infty s n(s) \tag{2.3}$$

and the mean number of trees destroyed by a lightning strike is

$$\bar{s} = \sum_1^\infty s^2 n(s)/\rho_t. \tag{2.4}$$

Since $\lim_{f/p\to 0} \rho_t$ is finite and $\bar{s}$ diverges as $(f/p)^{-1}$, these equations imply that $n(s)$ decreases at least like s^{-2} but not faster than s^{-3}. As long as the system is not exactly at the critical point $f/p = 0$, i.e. for non-vanishing f/p, there must be a cut-off in the cluster size distribution for very large forest clusters. We conclude that [14]

$$n(s) \propto s^{-\tau} \mathcal{C}(s/s_{\max}) \tag{2.5}$$

with $2 \leqslant \tau \leqslant 3$ and

$$s_{\max} \propto (f/p)^{-\lambda} \propto \bar{s}^{\lambda}. \tag{2.6}$$

The cut-off function $\mathcal{C}(x)$ is essentially constant for $x \leqslant 1$ and decreases to zero for large x. Equations (2.4)–(2.6) yield $\bar{s} \propto s_{\max}^{3-\tau}$, which leads to the scaling relation

$$\lambda = 1/(3-\tau). \tag{2.7}$$

In the case $\tau = 2$, the right-hand side of equation (2.5) acquires a factor $1/\ln(s_{\max})$, since the forest density given by equation (2.3) must not diverge in the limit $f/p \to 0$. The mean number of forest clusters per unit volume $\sum_1^\infty n(s)$, therefore, decreases to zero for $f/p \to 0$, and consequently the forest density approaches the value 1. This situation occurs in one dimension.

We also introduce the cluster radius $R(s)$ (radius of gyration) which is the mean distance of the trees in a cluster from their centre of mass. It is related to the cluster size s by

$$s \propto R(s)^{\mu}$$

with the fractal dimension μ.

The correlation length ξ is defined by

$$\xi^2 = \frac{2\sum_1^\infty s n(s) s R^2(s)}{\sum_1^\infty s n(s) s} \propto (f/p)^{-2\lambda/\mu}.$$

We conclude

$$\xi \propto (f/p)^{-\nu} \text{ with } \nu = \lambda/\mu. \tag{2.8}$$

In percolation theory, the *hyperscaling relation*

$$d = \mu(\tau - 1) \tag{2.9}$$

is satisfied, but it is not satisfied in the SOC FFM in $d = 2$, as first stated in [25], where also an interpretation of this relation is given: if equation (2.9) is satisfied, every box of $l^d \gg 1$ sites contains a spanning piece of a large cluster when the system is at the critical

point. In the FFM, there are at least in $d = 2$ many regions which contain no large forest cluster (see figure 4), and consequently $d < \mu(\tau - 1)$.

The mean forest density ρ_t approaches its critical value $\rho_t^c = \lim_{f/p \to 0} \rho_t$ via a power law

$$\rho_t^c - \rho_t \propto (f/p)^{1/\delta}. \tag{2.10}$$

One can also introduce several dynamical quantities and corresponding exponents characterizing the temporal behaviour of the fire (see [26]). Here, we mention only the time $T(s_{\max}) \propto (f/p)^{-\nu'}$ which it takes to burn down a cluster of size $s_{\max}$.

2.2. Simulation results

In this subsection, the simulation results for the critical exponents of the FFM are presented and discussed.

2.2.1. Critical exponents In one dimension, the critical exponents were determined not only by computer simulations, but also analytically [27] (See also subsection 2.3.2). In higher dimensions one has to resort to computer simulations. The model is simulated most effectively with a method first proposed in [28], which iterates the following rules:

1. Choose an arbitrary site in the system. If it is not occupied by a tree, proceed with rule 2. If it is occupied by a tree, then ignite the tree and burn down the forest cluster to which the tree belongs. While burning the trees, evaluate the properties of the cluster as size, radius, etc. Proceed with rule 2.
2. Choose p/f arbitrary sites in the system and grow a tree at all chosen empty sites. Proceed with rule 1.

By these rules, time scale separation is perfectly realized, and equation (2.1) is satisfied. In order to assure that the system is in the steady state, a sufficiently large number of time steps have to be discarded in the beginning of each simulation. In the following, we discuss the simulation results obtained for the critical exponents and the critical forest density.

The exponent τ is determined by measuring the cluster distribution $n(s)$ or the fire distribution $sn(s)$, which gives $\tau - 1$. In $d = 2$, $\tau \approx 2.15$, as found in [25, 26, 28, 29]. With increasing dimension, τ increases, too [29, 26], and assumes its mean-field value 2.5 in dimensions larger than 6 [26] (for simulation results see figure 5, and for a complete list of the values see table 1).

Reliable results for the exponent λ can be achieved by considering the normalized integrated distribution function $P(s) = \int_s^\infty \mathrm{d}s' s' n(s')$, which was first introduced in [28]. By collapsing different curves of $P(s)$ for different values of f/p , λ is found to be ≈ 1.16 [25, 26].

The critical forest density is $\rho_t^c \approx 0.41$ in $d = 2$ [25, 26, 28, 29], and it decreases with increasing dimension [29, 26]. Table 1 lists the results obtained in [26], where the system size was larger than in [29]. The exponent $1/\delta$ is ≈ 0.5 in $d = 2$[26, 28, 29].

The fractal dimension μ of the forest clusters is obtained from the slope of the cluster radius $R(s)$ (see figure 6). In 2 dimensions $\mu \approx 1.96$ [25, 26], which is smaller than 2, in contrast to earlier assumptions [14, 28]. The values in higher dimensions are given in table 1 [26] and seem to approach the mean-field value 4, which is supposedly exact above 6 dimensions. The hyperscaling relation equation (2.9) is definitely violated in $d = 2$ (see [25] for an interpretation), but cannot be ruled out from simulation results in higher dimensions.

Table 1. Numerical results for the critical exponents in 1 to 8 dimensions (* = with logarithmic corrections, † = calculated from scaling relations), taken from [26]. The exponents with index 'perc' are those of percolation theory [33].

d	1	2	3	4	5	6	7	8
L	2^{20}	16384	448	80	32	20	12	8
τ	2	2.14(3)	2.23(3)	2.36(3)	2.45(3)	2.50(3)	2.50(3)	2.50(3)
τ_{perc}	2	2.05	2.18	2.31	2.41	2.5	2.5	2.5
λ	1*	1.15(3)	1.30(6)	1.56(8)†	1.82(10)†	2.01(12)†	2.01(12)†	2.01(12)†
$1/\delta$	0*	0.48(2)	0.55(12)	——	——	——	——	——
ρ_t^c	1	0.4081(7)	0.2190(6)	0.146(1)	0.111(1)	0.090(1)	0.076(1)	0.066(1)
μ	1	1.96(1)	2.51(3)	3.0	3.2(2)	——	——	——
μ_{perc}	1	1.90	2.53	3.06	3.54	4	4	4
ν	1*	0.58	0.52(3)†	0.53(3)†	0.57(7)†	——	——	——
ν'	1*	0.58	0.64(6)†	0.78(8)†	0.92(10)†	1.04(11)†	1.05(11)†	1.05(11)†

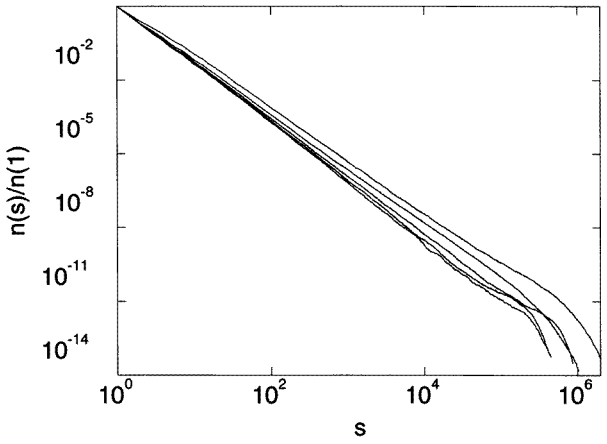

Figure 5. Normalized cluster size distribution $n(s)/n(1)$ for $d = 2$ to 6 dimensions. The values of f/p are 1/32000, 1/2000, 1/1000, 1/250 and 1/125 from right to left. The exponent τ is given by the negative slope.

The correlation length ξ is dominated by large clusters and consequently large radii. Therefore, the exponent ν could be directly determined only in $d = 2$ dimensions, with the result $\nu \approx 0.58$ [25, 26, 28]. The temporal analogon to the correlation length is $T(s_{\max}) \propto (f/p)^{-\nu'}$, with $\nu' \simeq 0.61$ in $d = 2$ [26].

All these simulation results for the critical exponents suggest that the SOC forest-fire model has an upper critical dimension $d_c = 6$, above which the critical exponents are identical with those of mean-field-theory, which again is identical to the mean-field-theory of percolation [29]. The strongest evidence for this behaviour comes from the exponent τ, which approaches the percolation value $\tau_{\text{perc}} = 5/2$ for $d \to 6$ and is indistinguishable from $5/2$ in all simulated dimensions $d \geqslant 6$. But also in the other exponents the difference between forest-fire and percolation values seems to vanish with increasing dimension.

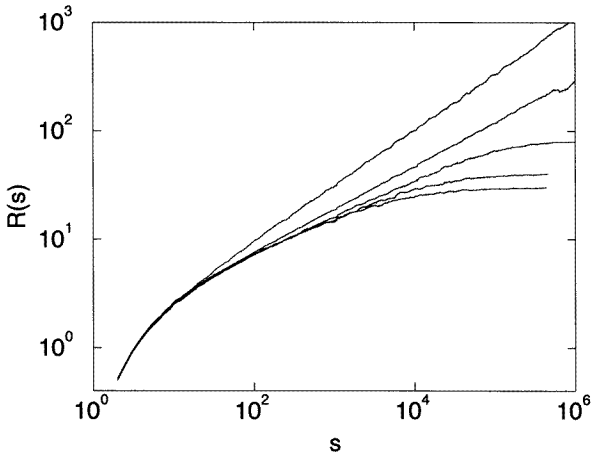

Figure 6. Cluster radius $R(s)$ in 2 to 6 dimensions (from left to right). The inverse slope yields the fractal dimension μ.

2.2.2. Universality In equilibrium systems, the critical behaviour usually depends only on properties as dimension and conservation laws, but not on microscopic details. It can therefore be expected that also the critical behaviour of the SOC FFM is universal under certain changes of the model rules. This assumption was checked in [26], where the 2D simulations were carried out for a triangular lattice ($\rho_t^c \approx 34\%$) and for a square lattice with next-nearest-neighbour interaction ($\rho_t^c \approx 28\%$). The critical exponents of these variations of the model were found to be the same. See, for instance, figure 7, where the correlation length for the three models is plotted. The critical densities are smaller than for the square lattice, since the fire has more possible paths to spread due to the larger number of neighbours.

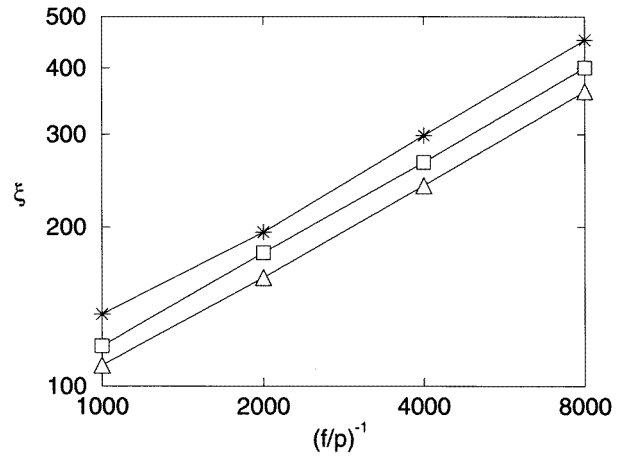

Figure 7. The correlation length ξ as function of $(f/p)^{-1}$. The slope yields the critical exponent ν. (□ = square lattice, △ = triangular lattice, ∗ = next-nearest-neighbour interaction.)

2.2.3. Immunity Another modification of the model rules is obtained by including a non-zero immunity g [30]. In contrast to the rule given in section 1, the simulations were performed with immune bonds instead of immune sites. Not all trees that are neighbours of a burning tree catch fire, and consequently the fire no longer burns forest clusters but clusters of trees that are connected by non-immune bonds. A small value of immunity corresponds essentially to a change in the lattice symmetry, since the effective coordination number is decreased. As we have just seen, a change of the lattice symmetry does not affect the critical exponents, which is again confirmed by the simulations. With increasing immunity, the forest density increases until the critical forest density becomes $\rho_t^c = 1$ at a critical immunity g_c. Here, a new scenario occurs: the forest is completely dense in the limit $f/p \to 0$, and clusters that are destroyed by fire are percolation clusters of bond percolation. Consequently, the exponents $\tau_c = \tau(g = g_c)$ and μ_c are given by percolation theory, and the threshold is $g_c = 1/2$, which is 1 minus the bond percolation threshold. Since the critical forest density is 1 at $g = g_c$, scaling relation equation (2.7) now reads

$$\lambda_c = \gamma_c/(3 - \tau_c) \tag{2.11}$$

with a new exponent γ_c.

For finite f/p, the mean forest density is no longer 1, and one can determine also the other critical exponents λ_c, δ_c, ν_c, and γ_c. The scaling relations equations (2.11) and (2.8) are confirmed by the simulations. Using equations (2.1) and (2.10), one obtains a new scaling relation $\bar{s} \propto (f/p)^{-\gamma_c}$ with $\gamma_c = 1 - 1/\delta_c$, which is also confirmed by the simulations.

When the immunity is just below its critical value g_c, a crossover from percolation-like to SOC behaviour is observed. On length scales smaller than the percolation correlation length $\xi_{\text{perc}} \propto (g_c - g)^{\nu_{\text{perc}}}$, a system close to the percolation threshold cannot be distinguished from a system exactly at the percolation threshold. As long as f/p is so large that fires do not spread further than ξ_{perc}, the exponents are identical to those at $g = g_c$. When f/p becomes very small, there are fires which spread further than the percolation correlation length. These fires are stopped by empty sites that were created by earlier fires. This is the same mechanism as for small g: fires that would spread indefinitely if there were no empty sites are stopped by empty sites. We conclude that these large fires lead to the critical exponents λ, ν, and δ that have been observed for $g = 0$. We make the following scaling *ansatz* for the correlation length:

$$\xi = (f/p)^{-\nu_c} F\left(\frac{g_c - g}{(f/p)^{\phi}}\right). \tag{2.12}$$

It is plausible that the crossover from percolation-like to SOC behaviour takes place when f/p becomes so small that the correlation length exceeds the percolation correlation length, which suggests that the crossover exponent ϕ is given by $\phi = \nu_c/\nu_{perc}$. The scaling function $F(x)$ is constant for small x and is $\propto x^{(\nu - \nu_c)/\phi}$ for large x. Analogous scaling laws hold for $s_{\max}$ and $\rho_t^c - \rho_t$. figure 8 shows the simulation results for the scaling function of the correlation length $F(x)$ for different values of $g_c - g$. The scaling *ansatz* equation (2.12) is well confirmed since all curves coincide. The dashed line represents $F(0)$ as obtained from the simulations at g_c. This crossover is similar to crossover phenomena at equilibrium phase transitions, and it should be observed also in higher dimensions. Although the crossover in τ and μ vanishes in dimensions larger than 6, there is still a crossover in λ and ν, due to the modified scaling relation at g_c. In $d = 1$, the critical immunity is $g_c = 0$, and no crossover can take place.

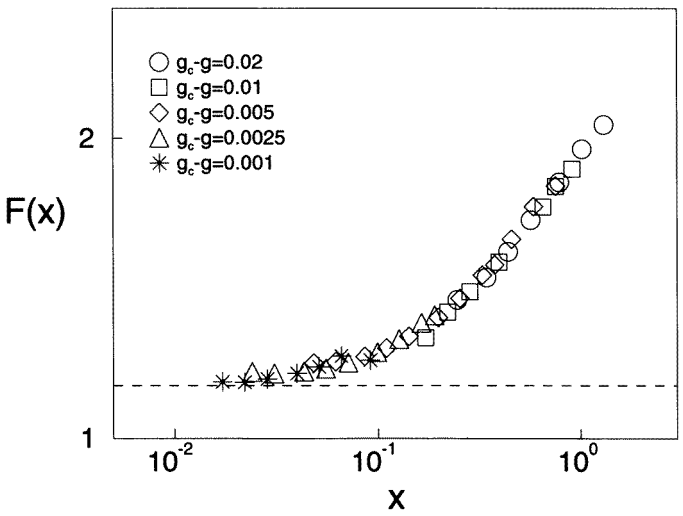

Figure 8. Crossover scaling function $F(x)$ for the correlation length for different values of the immunity. The dashed line represents $F(0)$ as obtained at $g = g_c$.

2.3. Analytical results

In this subsection, we review several analytical approaches to the SOC forest-fire model. First, we present the mean-field theory (MFT) which leads to the same exponents as the MFT of percolation. Then, we give several exact results for the one-dimensional model. Finally, we discuss attempts to establish a renormalization group for the forest-fire model.

2.3.1. Mean-field theory One of the simplest possible analytical approaches to a model is a MFT, which neglects all correlations in the system and describes it entirely in terms of densities. The neglect of correlations can be modelled in simulations by constructing a random-neighbour model, where the nearest-neighbour connections are chosen randomly at each time step [29]. The probability that a randomly chosen neighbour of a given burning tree is occupied by a green tree is obviously given by the tree density. In the stationary state, the mean-field equations are the following [29, 31, 32]:

$$\rho_f = p\rho_e \tag{2.13}$$

$$\rho_f = \rho_t \left(f + (1-f)(1-(1-\rho_f)^{2d})\right) \tag{2.14}$$

$$\rho_e + \rho_t + \rho_f = 1. \tag{2.15}$$

The first and last equations are exact (see equations (1.1) and (1.2)), since they involve no nearest-neighbour interactions. The second equation includes a mean-field approximation, since the probability that one or more neighbours of a given site are burning is given by $(1-(1-\rho_f)^{2d})$, without taking into account any correlations.

From these equations, we find an implicit equation for the fire density alone

$$\rho_f = \left(1 - \rho_f\,(1+1/p)\right)\left(1-(1-f)\,(1-\rho_f)^{2d}\right). \tag{2.16}$$

In the SOC limit, p, f, and ρ_f are very small compared to 1, and we find to leading order

$$\rho_f = p(1-1/2d) + f/2d + O(p^2, pf, \cdots) \tag{2.17}$$

$$\rho_e = 1 - 1/2d + f/2dp + O(p, f, \cdots) \tag{2.18}$$

$$\rho_t = 1/2d - f/2dp + O(p, f, \cdots). \tag{2.19}$$

The tree density approaches its critical value linearly in f/p, leading to $\delta = 1$. The critical tree density is $\rho_t(f/p = 0) = 1/2d$, which means that a burning tree ignites on an average just one other tree. This situation is identical to MFT of percolation or, equivalently, percolation on a Cayley tree, where percolation proceeds to each available neighbour with the same probability and to one neighbour on an average. The cluster size distribution and the fractal dimension of clusters for this problem are well known [33]. We therefore obtain $\tau = 2.5$ and $\mu = 4$. Scaling relations equations (2.7) and (2.8) then give $\lambda = 2$ and $\nu = 0.5$. Percolation has the upper critical dimension 6, and one might expect that the SOC forest-fire model has the same upper critical dimension, as conjectured in [26, 28, 29] and supported by the simulation results (see subsection 2.2).

When the limit $p \to 0$ with $f = 0$ is considered instead of the limit $f \to 0$ with $p \ll f/p$, the MFT of the forest-fire model also gives a critical tree density $1/2d$, leading again to the same exponents as MFT of percolation. In MFT the structural information is lost and thus MFT cannot see the qualitative difference between the SOC state and the quasideterministic state with spiral-shaped fire fronts.

2.3.2. Exact results in one dimension In one dimension, exact results have been obtained in [27, 31, 34], thus proving analytically that non-conservative models can indeed show SOC. Here, we give an intuitive derivation of the results. Consider a string of $k \ll p/f$ sites. This string is too short for two trees to grow during the same time step. Lightning does not strike this string before all of its trees are grown. Since we are always interested in the limit $f/p \to 0$, the following considerations remain valid even for strings of a very large size. Starting with a completely empty string, it passes through a cycle which is illustrated in figure 9. During one time step, a tree grows with probability p on any site. After some time, the string is completely occupied by trees. Then the forest in the neighbourhood of the string will also be quite dense. The trees on the string are part of a forest cluster which is much larger than k. Eventually that cluster becomes so large that it is struck by lightning with a non-vanishing probability. Then the forest cluster burns down, and the string again becomes completely empty.

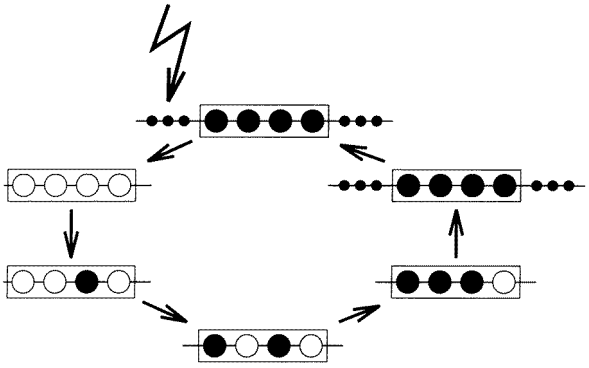

Figure 9. Dynamics on a string of $k = 4$ sites. Trees are black, empty sites are white.

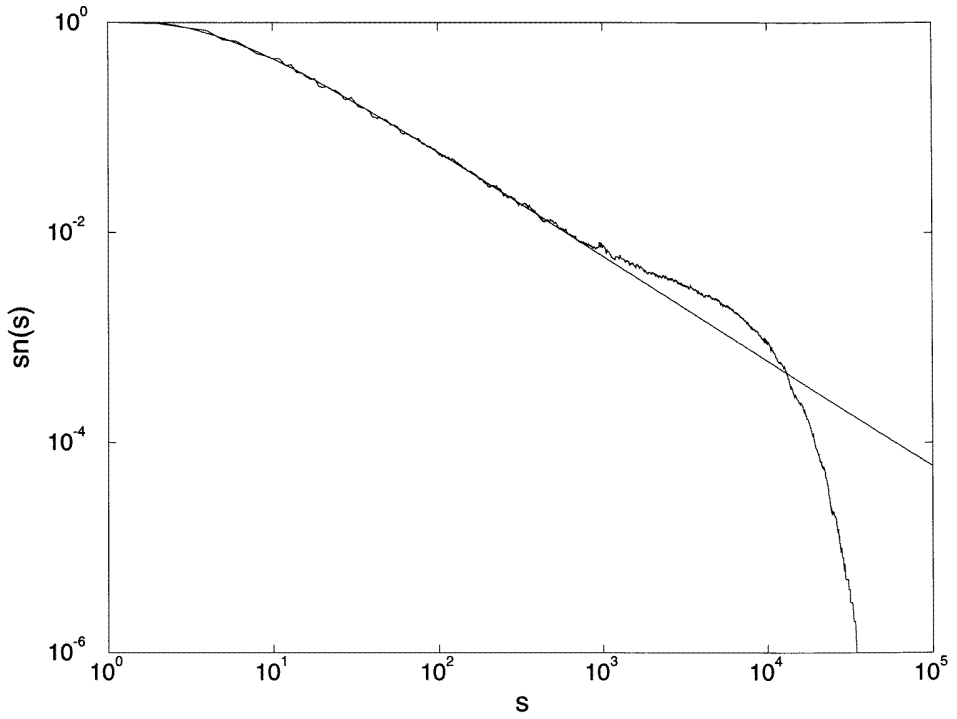

Figure 10. Size distribution of the fires for $d = 1$, $f/p = 1/25000$ and $L = 2^{20}$. The smooth line is the theoretical result which is valid for cluster sizes $\leqslant s_{\max}$.

This consideration allows us to write down rate equations for the states of the string. In the steady state, each configuration of trees is generated as often as it is destroyed. Let $P_k(m)$ be the probability that the string is occupied by m trees. Each configuration which contains the same number of trees has the same probability. A configuration of m trees is destroyed when a tree grows at one of the empty sites, and is generated when a tree grows in a state consisting of $m-1$ trees. The completely empty state is generated when a dense forest burns down. Since all trees on our string burn down simultaneously, this happens each time when a given site of the string is set on fire. This in turn happens as often as a new tree grows at this given site, i.e. with probability $p\,(1-\rho_t)$ per time step. We therefore have the following equations,

$$pkP_k(0) = p\,(1-\rho_t) \tag{2.20}$$

$$p(k-m)P_k(m) = p\,(k-m+1)P_k(m-1) \qquad \text{for } m \neq 0, k. \tag{2.21}$$

We conclude

$$P_k(m) = (1-\rho_t)/(k-m) \quad \text{for } m < k \tag{2.22}$$

$$P_k(k) = 1-(1-\rho_t)\sum_{m=0}^{k-1} 1/(k-m) = 1-(1-\rho_t)\sum_{m=1}^{k} 1/m. \tag{2.23}$$

These last two equations contain a wealth of information: cluster size distribution, hole distribution, growth velocity etc.

A forest cluster of size s is a configuration of s neighbouring trees with an empty site at each end. The size distribution of forest clusters is consequently given by

$$n(s) = \frac{P_{s+2}(s)}{\binom{s+2}{s}} = \frac{1-\rho_t}{(s+1)(s+2)} \simeq (1-\rho_t)s^{-2}. \tag{2.24}$$

This is a power law with the critical exponent $\tau = 2$. The size distribution of fires is $\propto sn(s) \propto s^{-1}$. Figure 10 shows the numerical result for the fire distribution $sn(s)$. It agrees perfectly with equation (2.24) in the region $s < s_{\max}$.

$s_{\max}$, introduced in equations (2.5) and (2.6) is the characteristic size (in one dimension length) where the power law $n(s) \propto s^{-2}$ breaks down. We calculate $s_{\max}$ from the condition that a string of size $k \leqslant s_{\max}$ is not struck by lightning until all trees are grown. When a string of size k is completely empty at time $t = 0$, it will be occupied by k trees after

$$T(k) = (1/p)\sum_{m=1}^{k} 1/m \simeq \ln(k)/p$$

time-steps on an average. The mean number of trees after t time-steps is

$$m(t) = k[1 - \exp(-pt)].$$

The probability that lightning strikes a string of size k before all trees are grown is

$$f\sum_{t=1}^{T(k)} m(t) \simeq (f/p)k(\ln(k) - 1) \simeq (f/p)k\ln(k).$$

We conclude

$$s_{\max}\ln(s_{\max}) \propto p/f \quad \text{for large } p/f$$

leading to $\lambda = 1$.

Next we determine the relation between the mean forest density ρ_t and the parameter f/p. The mean forest density is given by

$$\begin{aligned}\rho_t &\simeq \sum_{s=1}^{s_{\max}} sn(s) \\ &= (1-\rho_t)\sum_{s=1}^{s_{\max}} \frac{s}{(s+1)(s+2)} \\ &\simeq (1-\rho_t)\ln(s_{\max}).\end{aligned}$$

Thus

$$\frac{\rho_t}{1-\rho_t} \simeq \ln(s_{\max}) \simeq \ln(p/f) \quad \text{for large } p/f.$$

The forest density approaches the value 1 at the critical point. This is not surprising since no infinitely large cluster exists in a one-dimensional system as long as the forest is not completely dense.

The exponents characterizing the size distribution of forest clusters and fires remain the same when the fire is allowed to jump over holes of several empty sites [35], proving the universality of the critical exponents. A change in the range of the interaction corresponds to a change in lattice symmetry in higher dimensions, where universality also has been found (see subsection 2.2).

The values of the exponents change, however, when the rule for tree growth is modified. When tree growth becomes more deterministic, the critical behaviour eventually breaks down, and the system becomes synchronized [36]. To illustrate this, let us look at the

case of completely deterministic tree growth, where an empty site turns to a tree exactly T time steps after the site has become empty. Neighbouring sites, both of which happen to be occupied by a tree, burn down during the same fire. They consequently turn to trees simultaneously and burn down together simultaneously for all future times, i.e. they are synchronized. After some time, the system will consist of synchronized blocks which are so large that they are struck by lightning before the neighbouring blocks become occupied by trees.

As an intermediate case, let us next consider a tree growth rule where the lifetime distribution of empty sites is a constant $1/T$ over a time T. An initially empty string of k sites then grows the same number of trees during each time step, irrespective of the number of occupied sites. The string consequently becomes occupied after a finite time. The above-mentioned deterministic model is just a coarse-grained version of this model, and we therefore expect that the system is dominated by large fires. Due to stochastic tree growth, however, there exist also small forest clusters. At small scales k, we find that $P_k(m)$ has the same value for all $m < k$, leading to $n(s) \propto s^{-3}$. The simulation results figure 11 show this power law for small cluster sizes, and the expected peak at large clusters, indicating synchronization. When the distribution of lifetimes of empty sites has a power-law tail, the system shows SOC behaviour with an exponent which depends on the exponent characterizing the tail [36].

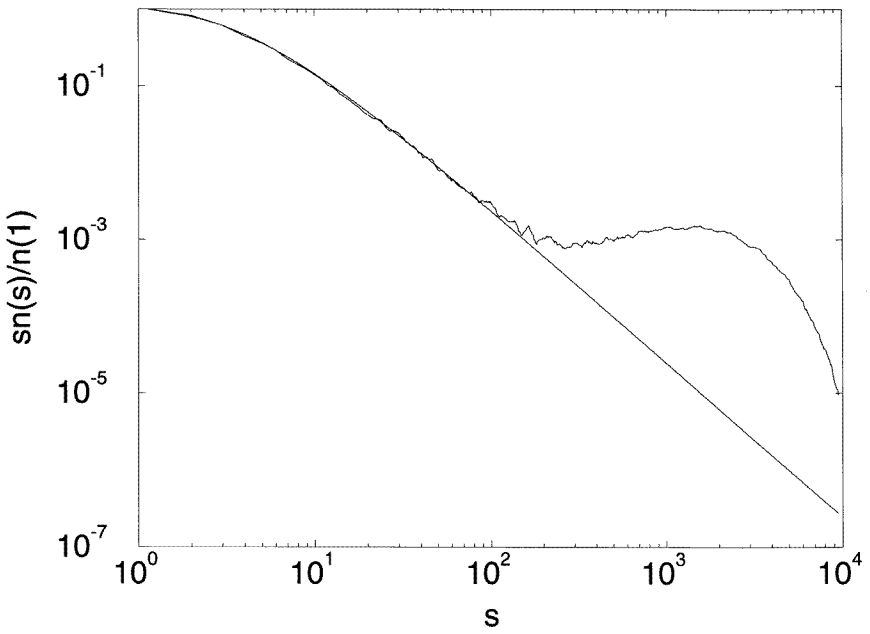

Figure 11. Normalized size distribution of fires in a version where the lifetime distribution of empty sites is a constant function $P(\tau) = 1/100$ for times $\tau < 100$. The parameters are $L = 10000$ and $f = 0.00001$. The smooth line is the theoretical result, which is valid for $s \leqslant s_{\max}$.

2.3.3. Renormalization group approach In equilibrium critical phenomena, the invariance of the system under a change of length and time scale together with a partial trace operation

leads to a renormalization group (RG) approach. A RG not only yields values (possibly approximate, if one has to use perturbation theory) for the critical exponents in low dimensions, but also information on the upper critical dimension and on universality classes.

The separation of time scales and the avalanche structure of the forest-fire model and other SOC models make it difficult to find an appropriate RG formalism for these systems. Two approaches which have been taken so far [37, 38] do not yet discriminate between the two limits $\lim_{p\to 0}\lim_{f\to 0}$ and $\lim_{f\to 0}$ with $p \ll (f/p)^{\nu'}$. The real-space RG in [37], which neglects correlations, yields the correct exponents in one dimension, and good approximations in two dimensions. In [38], the FFM is mapped on a field theory, but the subsequent calculations contain severe approximations. In a third approach [39], the forest-fire model is also mapped on a field theory. However, the renormalization in the limit of double time scale separation remains a problem.

3. Modifications of the forest-fire model

The forest-fire model can be modified in many ways, and some of these modifications show very interesting behaviour. A version with conserved tree density is suggested in [31] and studied in [40]. After each fire, all trees which have been burnt are regrown at randomly chosen empty sites. For tree densities smaller than ρ_t^c, this model has only finite fires and can be mapped on the SOC forest-fire model by finding the corresponding value of f/p. For densities between $\rho_t^c \simeq 0.41$ and a second critical density $\rho_t^{c2} \simeq 0.435$, the system shows critical behaviour with a power-law size distribution of fires and of tree clusters. Both the cut-off in cluster size and the correlation length diverge with some power of the system size (see figure 12). The exponents depend on the density. Thus one has the interesting situation that criticality is not confined to a point but exists in a finite interval. For even higher average density, the system splits into several subphases with different densities (figure 13). The subphase with highest density contains an infinite cluster. The number of subphases which can be sustained depends on the system size, and their shape on the boundary conditions. Another modification of this model, where each tree is grown immediately after it has been burnt, shows both critical behaviour and spiral-shaped fire fronts [41].

A deterministic version of the forest-fire model with continuous tree growth has been suggested in [42]. The variable 'tree height' is increased globally and very slowly. Trees higher than a certain threshold catch fire and ignite all neighbours above a second, smaller, threshold. The height of the tree after the fire is a function of the height before the fire [43]. studies a generalized version and shows that this model is not critical, but shows periodic behaviour or finite fires, depending on the value of a parameter. Another continuous model, which additionally includes energy diffusion, shows small or large fires, depending on the parameters, and the two regimes are separated by a critical point [44].

4. A selection of other SOC models

Many systems have been introduced as examples for SOC. For part of these systems, the evidence is based on numerical data for relatively small system sizes with little analytical understanding of the origin of the critical behaviour. In this section, we discuss three of the most thoroughly studied SOC models and compare them with the forest-fire model. Although the term SOC has been used in many different contexts, we restrict ourselves to systems with slow driving (energy input) and dissipation events which are instantaneous on

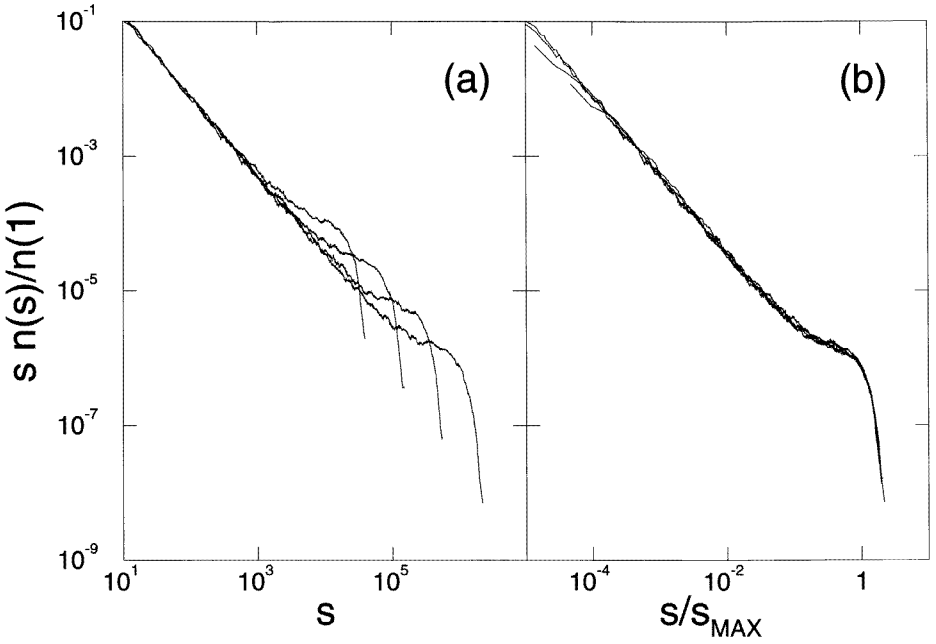

Figure 12. Normalized size distribution of fires in the model with tree conservation, for $\rho = 0.43$ and L = 512, 1024, 2048, 4096, (a) before and (b) after rescaling.

the time scale of driving. The size distribution of dissipation events obeys a power law. Further examples for SOC include the dynamics of magnetic domain patterns [45, 46], cloud formation [12], evolution of populations [10, 11], erosion [13], fracture [47], fragmentation [48], the Bean critical state in type II superconductors [49], depinning transitions of interfaces, charge density waves or superconducting flux lattices [50], and many more. Although not treated in this section, these examples underline the importance of SOC as a crossdisciplinary subject with applications in physics, biology, chemistry and geology.

4.1. Sandpile model

The sandpile model is the prototype for SOC [5, 6]. Sand grains are dropped at random on the sites of a lattice. When the number of grains on a lattice site ('height model') or the difference in the grain number between neighbours ('slope model') exceeds a certain threshold, the site topples and redistributes its grains amongst the nearest neighbours. When a neighbour thereby is lifted above the threshold, it topples too, and the avalanche continues until all sites are below or at the threshold. Then a new grain of sand is added at random. In the stationary state, the mean number of added grains must equal the mean number of grains leaving the system at the edge, and there must exist avalanches spreading over a distance of the order of the system size. The sandpile therefore is in a critical state where sand grains are redistributed on all scales. For the height model, several exact results have been obtained [51]. The critical state is robust with respect to a variety of changes, but is usually destroyed when the local conservation law is violated. Real sandpiles behave differently, mainly because large avalanches have large inertia and are not immediately stopped when the slope becomes small.

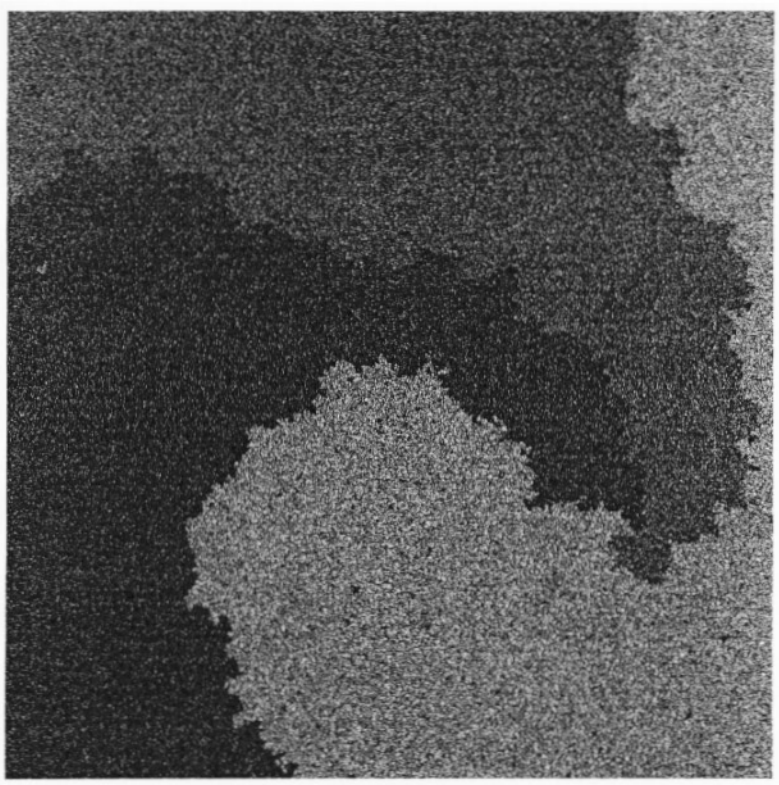

Figure 13. Stationary state in the model with tree conservation for $\rho = 0.50$, $L = 2048$ and absorbing boundary conditions (trees are black, empty sites are white).

In contrast to the forest-fire model, the sandpile model has only two separated time scales. The condition that avalanches relax before new grains of sand are added, corresponds to the condition that a fire is extinguished before new trees grow. In the sandpile model, large avalanches occur due to the local conservation of sand grains, in the forest-fire model large fires occur in the limit $f/p \to 0$. It has been pointed out in [37] that the sandpile model can be simulated exactly at the critical point, while the forest-fire model is only close to its critical point and has therefore a relevant parameter. However, in any realistic physical situation, the driving rate for the sandpile model can never be exactly equal to zero, resulting also in a relevant parameter and an upper cut-off in avalanche size. Above that size, avalanches overlap.

4.2. Earthquake model

The earthquake model [8] is a continuous, non-conservative variant of the sandpile model. It can be derived from a 2D spring-block model for the motion of tectonic plates (Burridge–Knopoff model). The force on all sites ('blocks') is increased uniformly and very slowly. When the force at a given site exceeds a threshold, the block moves to its equilibrium position, and the force on the corresponding site is reset to zero. The force on the 4 nearest neighbours is increased by a fixed percentage of the released force. This percentage depends on the ratio of the spring constants in the model, and is usually smaller than 1/4,

i.e. the model has no conservation law. The system is not driven as long as there are forces above the threshold and an 'earthquake' is going on. The size distribution of earthquakes is found to obey a power-law, in agreement with the famous Gutenberg–Richter law for the size distribution of real earthquakes. The exponent depends continuously on the degree of conservation, and the critical behaviour seems to persist even in the limit where almost no force is transmitted to the neighbours. The size of the largest avalanche diverges with diverging system size, but so slowly that it covers only a vanishing part of the system [52, 53]. When the global driving is replaced by local driving, when inhomogeneities such as defects are present, or when the open boundary conditions are replaced by boundary conditions, the critical state is destroyed [54]. The authors of [54] show that the critical behaviour is related to a partial synchronization of neighbouring sites. However, the origin of the critical behaviour of the earthquake model, and in particular the dependence of the critical exponents on the degree of conservation, is relatively poorly understood. A similar behaviour has been found so far only in one other model, namely the above-mentioned version of the forest-fire model with tree conservation [40].

In this context, another earthquake model that is also derived form the Burridge–Knopoff model, is worth mentioning [55]. Like the above model, it is deterministic and continuous, but additionally it includes effects of inertia. It shows a power-law size distribution over a certain range of earthquake sizes, but the very large earthquakes occur more frequently than expected from a power-law distribution, and in periodic time intervals. From the evaluation of earthquake data, it is not obvious, which of the two models is more appropriate.

4.3. Evolution model

A particularly simple SOC model is the so-called 'evolution model' [11]. Each site in a one-dimensional chain is assigned a random number between 0 and 1 ('fitness'). The probability for a 'mutation' depends exponentially on the fitness, and in the zero-temperature limit the site with smallest fitness is always mutated. This site is assigned a new random number between 0 and 1. Since a mutation at one site affects the fitness of the neighbours, the two nearest neighbours are also assigned new random numbers. After some time, only a vanishing percentage of all sites have a fitness below a threshold $\simeq 0.67$. A mutation of a site at the threshold releases an avalanche of mutations which is stopped when no site is below the threshold any more. The size distribution of these avalanches obeys a power law. A review of the properties of this and related models and of some exact results is given in [50].

Reference [50] also mentions a less spectacular application of this model, namely the depinning of interfaces, which usually occurs when a driving force exceeds a certain threshold. When not the driving force, but the interface velocity is chosen to be the parameter, the depinning transition becomes SOC in the limit of zero velocity [56, 57, 58], which is again a separation of time scales.

5. Conclusions

The main part of this review was devoted to the forest-fire model as a simple example for driven, dissipative systems with many degrees of freedom. Depending on the value of the parameters, the model shows fundamentally different structures. One finds a quasi-deterministic state with spiral waves, percolation-like behaviour and, in particular, a self-organized critical state in the limit of double time scale separation. The properties of the SOC state have been analysed numerically and analytically. The critical behaviour has been

shown to be very robust with respect to a variety of changes of the rules of the model.

The notion of SOC has originally been introduced as a possible explanation for the ubiquity of fractal structures and $1/f$-noise in nature. Although this is a fascinating hypothesis, SOC seems to account only for the existence of part of these phenomena. Other extensively studied mechanisms producing fractals are diffusion-limited aggregation (DLA), kinetic roughening, and chaos and turbulence.

All SOC models presented in this paper have slow driving and avalanche-like dynamics. However, not all systems that show these two features are SOC. Besides a power-law size distribution of avalanches, such systems might also have many small avalanches which release only little energy, or only large avalanches which release a finite part of the system's energy, or some combination of both. SOC systems are naturally at the critical point, due to a conservation law (sandpile model), a second time scale separation (forest-fire model), a competition between open boundary conditions and the tendency of neighbouring sites to synchronize (earthquake model), or due to the slow driving alone (evolution model). However, the critical behaviour often breaks down when details of the model rules are changed, and is replaced by some other scenario. As examples we mentioned the forest-fire model with deterministic tree growth and the earthquake model with modified boundary conditions.

The forest-fire model is closely related to excitable media. So far, spiral waves, target patterns and chaotic behaviour have been found and investigated in excitable media. By investigating the appropriate parameter region one should also be able to find percolation-like behaviour and the self-organized critical state, which exist in the FFM. The SOC state should occur whenever there is spontaneous excitation that spreads very fast compared to the recovery time (e.g. fatal diseases, that occur seldom, but spread rapidly), provided that the probability distribution for the recovery time is not too narrow.

After many years of studying formation of structure in non-equilibrium systems, one has got a glimpse at the mechanisms producing the overwhelming variety and complexity of structures surrounding us in nature, and there are certainly still many exciting phenomena to be discovered.

References

[1] Mandelbrot B B 1983 *The Fractal Geometry of Nature* (New York: Freeman)
[2] Bunde A and Havlin S 1991 *Fractals and Disordered Systems* ed A Bunde and S Havlin (New York: Springer)
[3] Press W H 1978 *Comm. Astrophys.* **7** 103
[4] Dutta P and Horn P M 1981 *Rev. Mod. Phys.* **53** 497
[5] Bak P, Tang C and Wiesenfeld K 1987 *Phys. Rev. Lett.* **59** 381
[6] Bak P, Tang C and Wiesenfeld K 1988 *Phys. Rev.* A **38** 364
[7] Bak P and Creutz M 1994 *Fractals in Science* ed A Bunde and S Havlin (Berlin: Springer)
[8] Olami Z, Feder H J S and Christensen K 1992 *Phys. Rev. Lett.* **68** 1244
[9] Christensen K and Olami Z 1992 *Phys. Rev.* A **46** 1829
[10] Bak P, Chen K and Creutz M 1989 *Nature* **342** 789
[11] Sneppen K and Bak P 1993 *Phys. Rev. Lett.* **71** 4083
[12] Nagel K and Raschke E 1992 *Physica* A **182** 519
[13] Takayasu H and Inaoka H 1992 *Phys. Rev. Lett.* **68** 966
[14] Drossel B and Schwabl F 1992 *Phys. Rev. Lett.* **69** 1629
[15] Drossel B and Schwabl F 1993 *Physica* A **199** 183
[16] Tyson J J and Keener J P 1988 *Physica* D **32** 327
[17] Meron E 1992 *Phys. Rep.* **218** 1
[18] Bak P, Chen K and Tang C 1990 *Phys. Lett.* A **147** 297
[19] Grassberger P and Kantz H 1991 *J. Stat. Phys.* **63** 685
[20] Moßner W, Drossel B and Schwabl F 1992 *Physica* A **190** 205

[21] Greenberg J M and Hastings S P 1978 *Siam. J. Appl. Math.* **34** 515
[22] Albano E V 1995 *Physica* A **216** 213
[23] Johansen A 1994 *Physica* D **78** 186
Johansen A 1996 *J. Theor. Biol.* **178** 45
[24] Henley C L 1989 *Bull. Am. Phys. Soc.* **34** 838
[25] Henley C L 1993 *Phys. Rev. Lett.* **71** 2741
[26] Clar S, Drossel B and Schwabl F 1994 *Phys. Rev.* E **50** 1009
[27] Drossel B, Clar S and Schwabl F 1993 *Phys. Rev. Lett.* **71** 3739
[28] Grassberger P 1993 *J. Phys. A: Math. Gen.* **26** 2081
[29] Christensen K, Flyvberg H and Olami Z 1993 *Phys. Rev. Lett.* **71** 2737
[30] Drossel B, Clar S and Schwabl F 1994 *Phys. Rev.* E **50** R2399
[31] Drossel B 1994 *PhD Thesis* TU München
[32] Drossel B and Schwabl F 1194 *Physica* A **204** 212
[33] Stauffer D and Aharony A 1992 *Introduction to Percolation Theory* (London: Taylor and Francis)
[34] Paczuski M and Bak P 1993 *Phys. Rev.* E **48** R3214
[35] Drossel B, Clar S and Schwabl F 1994 *Z. Naturforsch.* **49** 856
[36] Drossel B 1996 *Phys. Rev. Lett.* **76** 936
[37] Loreto V, Pietronero L, Vespignani A and Zapperi S 1995 *Phys. Rev. Lett.* **75** 465
[38] Patzlaff H and Trimper S 1994 *Phys. Lett.* A **189** 187
[39] Bottani S and Delamotte B unpublished
[40] Clar S, Drossel B and Schwabl F 1995 *Phys. Rev. Lett.* **75** 2722
[41] Clar S, Schenk K and Schwabl F unpublished
[42] Chen K, Bak P and Jensen M 1990 *Phys. Lett.* A **149** 207
[43] Socolar J E S, Grinstein G and Jayaprakash C 1993 *Phys. Rev.* E **47** 2366
[44] Chan T C, Chau H F and Cheng K S 1995 *Phys. Rev.* E **51** 3045
[45] Che X and Suhl H 1990 *Phys. Rev. Lett.* **64** 1670
[46] Bak P and Flyvbjerg H 1992 *Phys. Rev.* A **45** 2192
[47] Bernardes A T and Moreira J G 1995 *J. Physique* I **5** 1135
[48] Oddershede L, Dimon P and Bohr J 1993 *Phys. Rev. Lett.* **71** 3107
[49] Tang C 1993 *Physica* A**194** 315
[50] Paczuski M, Maslov S and Bak P 1995 *Phys. Rev.* E
[51] Dhar D 1990 *Phys. Rev. Lett.* **64** 1613
[52] Janosi I M and Kertesz J 1993 *Physica* A **200** 179
[53] Grassberger P 1994 *Phys. Rev.* E **49** 2436
[54] Middleton A A and Tang C 1995 *Phys. Rev. Lett.* **74** 742
[55] Carlson J M and Langer J S 1989 *Phys. Rev. Lett.* **62** 2632
Carlson J M and Langer J S 1989 *Phys. Rev.* A **40** 6470
[56] Havlin S, Barabasi A L, Buldyrev S V, Peng C K, Schwartz M, Stanley H E and Vicsek T 1992 *Proc. Granada Conf., Spain (1991)* ed J M Garcia-Ruiz, E Louis, L Sander and P Meakin
[57] Sneppen K 1992 *Phys. Rev. Lett.* **69** 3539
[58] Zaitsev T 1992 *Physica* A **189** 411